

A Parameterized Model of Bolted Joints in Machine Tools

Hongqi Li and Bin Li

National NC System Engineering Research Center, Huazhong University of Science and Technology, Wuhan, 430074, China

Kuanmin Mao and Xiaolei Huang

State Key Laboratory of Digital Manufacturing Equipment and Technology, Huazhong University of Science and Technology, Wuhan, 430074, China

Fangyu Peng

National NC System Engineering Research Center, Huazhong University of Science and Technology, Wuhan, 430074, China

(Received 7 July 2012; provisionally accepted 4 April 2013; accepted 21 October 2013)

A new dynamic model for bolted joints in heavy machine structures is proposed. The influence of the bolt pre-tightening force, the interface dimensions and the surface roughness on joint dynamics (i.e. the stiffness matrix of finite element) were analysed. Each stiffness coefficient in the matrix can be expressed by an exponential function of preload, and a quadratic polynomial function of geometric dimensions. Sixteen specimens were thoroughly designed and analysed. Then, the resulting stiffness matrices were saved as templates, based on which could establish dynamic models of joints with different influence factor values, using curve-fitting and Response Surface Methodology (RSM). The methodology was validated by experiments with a specimen of the new design and a heavy-duty cutting machine.

1. INTRODUCTION

The characteristics of joints have significant influence on the dynamic performance of whole structures.¹ Research on the modelling and identification of joint stiffness has been conducted widely for machine structures. Yoshimura² proposed a dynamic model to analyse the joints between two components using an equivalent spring-damper system of six degrees of freedom. Greenwood³ modelled the joint dynamics with a normal spring, according to the Hertz contact theory. Some other researchers^{4,5} modelled the joint dynamics with a group of spring-dampers. Based on the Least Square Method, Tsai and Chou,⁶ as well as Wang and Ren et al.,^{7,8} extracted the joint dynamic parameters by analysing the Frequency Response Function (FRF). Ahmadian and Jalali^{2,3} formulated a non-linear generic element model for bolted lap joints by satisfying all known conditions for a joint interface, and hence provided a non-linear parametric formulation for the families of allowable joint models. According to the stiffness influence factor, a novel dynamic model of fixed joints was proposed by K. Mao and B. Li,⁹ which elaborated the identification of the model parameters in detail and verified its high accuracy through experiments.

Based on the study of the influence factors of joint dynamics, this paper presents a parameterized dynamic model of bolted joints, whose parameters can be calculated without additional experiments as long as the values of the involved influence factors (e.g., preloads, interface dimensions, and surface roughness) are known. Therefore, this study may be widely applied in industry.

This paper is organized as follows: Section 2 describes the

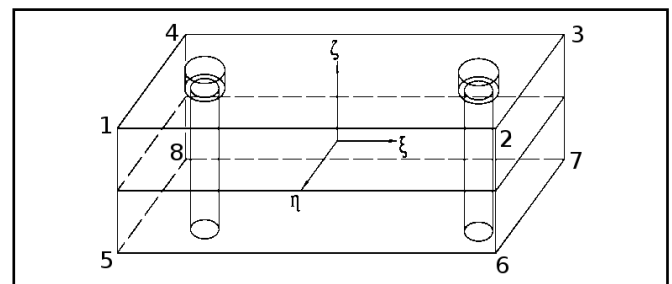


Figure 1: The bolted joint element.

effects of the preloads, the geometric dimensions, and the surface roughness on bolted joint dynamics. The sample database of joints is described in Section 3, with a detailed modelling process. In Section 4, the proposed model is experimentally validated with designed specimen and a heavy-duty cutting machine.

2. ANALYSIS OF THE EFFECT OF BOLTED-JOINT DYNAMICS

2.1. Introduction to the Influence Factors

Based on a wide investigation of manufacturing shops, a new model of bolted joint element with eight nodes was proposed by K. Mao et al.⁹ as shown in Fig. 1.

According to the definition of the stiffness influence factor, the model of the bolted joint element can be expressed as in Eq. 1, where $i, m = 1, 2, 3, 4$ represent the node; $j, n = 1, 2, 3$ represent the direction; and K_{mn}^{ij} is the stiffness influence coefficient. This correspond to the necessary force imposed on

$$\sum_{n=1}^3 K_{1n}^{ij}(x_{1n} - x_{5n}) + \sum_{n=1}^3 K_{2n}^{ij}(x_{2n} - x_{6n}) + \sum_{n=1}^3 K_{3n}^{ij}(x_{3n} - x_{7n}) + \sum_{n=1}^3 K_{4n}^{ij}(x_{4n} - x_{8n}) = f_{ij}. \quad (1)$$

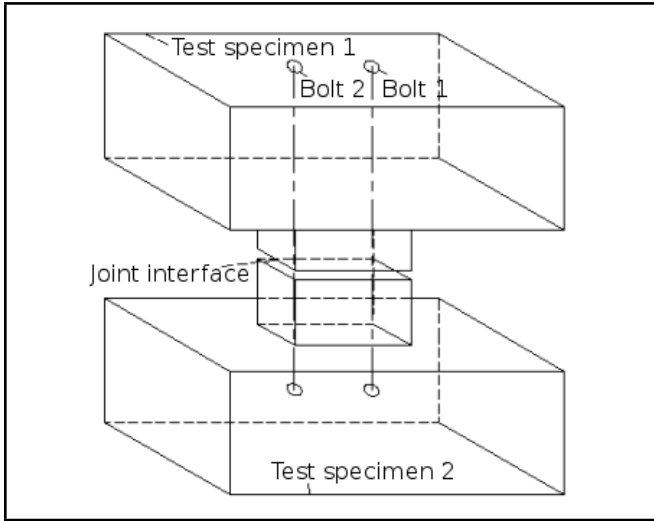


Figure 2: The test specimen.

node i in the j direction when the unit relative displacement is only generated in the direction of n of the node m and the node $(m + 4)$.

Under equilibrium conditions, there is:

$$f_{1j} = -f_{5j}, f_{2j} = -f_{6j}, f_{3j} = -f_{7j}, f_{4j} = -f_{8j}, j = 1, 2, 3.$$

Then, Eq. (1) can be written as:

$$[K]X = F; \quad (2)$$

where

$$X = (x_{11}, x_{12}, x_{13}, \dots, x_{81}, x_{82}, x_{83});$$

$$F = (f_{11}, f_{12}, f_{13}, \dots, f_{81}, f_{82}, f_{83});$$

$$[K] = \begin{pmatrix} K' & -K' \\ -K' & K' \end{pmatrix}_{24 \times 24};$$

and where $[K]$ is an asymmetric matrix, while $[K']$ is a 12×12 finite element stiffness matrix.

The dynamic equation of the fixed joint element can be obtained as follows:

$$(i\eta[K] + [K])X = F; \quad (3)$$

where η is the structural damping coefficient of the finite element, which is derived from the hysteretic loop of the force and the displacement.

For the precise identification of the matrix $[K]$, specimens with the shape shown Fig. 2 were manufactured and connected by given bolts. The design principle and rationality was described by Mao et al.⁹ Additionally, Fig. 3 shows the details of each substructure, where a , b , and $H = 45\text{mm}$ denote the length, width, and height of the convex platform; l , w and h are the block length, width, and height, respectively.

The stiffness matrices $[K]$ of the joint element of the manufactured specimen were identified through modal tests.⁹

Nevertheless, the matrix $[K]$, representing the dynamics of the joint element, is influenced by many factors that can be categorized into the three types listed below:

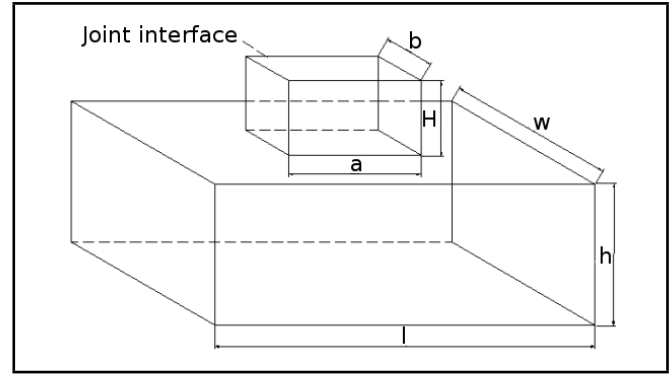


Figure 3: The substructure of the specimen.

- Type 1: relating to the structure factors of the joint configuration (linear or array), dimension, and shape
- Type 2: relating to the working conditions of the contact pressure, joint state, and state of the medium joint
- Type 3: relating to the joint material, the heat treatment process, the machining method, and the surface roughness.

For the actual bolted joint elements, it is expensive to design and manufacture the specimens that account for the actual preload, interface dimension, and surface roughness. It is also, time-consuming to conduct further modal tests. Therefore, this paper intends to develop a statistical model of the bolted joint element based on the test results of a finite number of specimens.

2.2. Influence of Preload on Dynamic Parameters

A large number of studies¹⁰ have shown that when the preload increases, along with the unchanged interface roughness and dimension, the stiffness of the joint elements increases with the descending slope. The relationship between each element of the stiffness matrix and the preload applied on the machine joints can be expressed as an exponential function. In this paper, such a function is presented as:

$$K_{ij} = cF^d; \quad (4)$$

where F is the positive preload and $K_{ij}(i, j = 1, 2, 3 \dots 24)$ is the element of the stiffness matrix $[K]$, and c and d are unknown parameters to be determined. In the following, Eq. (4) is regarded as a parameterized/statistical model of the dynamic stiffness influence coefficients K_{ij} .

For every stiffness coefficient K_{ij} , one can determine an exponential equation according to the coefficient's value with a finite number of different bolt pre-tightening forces. Hence, this equation can be used to determine the stiffness coefficient K_{ij} with any other bolt pre-tightening forces. According to the dynamic modelling and parameter identification methods established,⁹ the elements of the stiffness matrix, $K_{ij}(i, j = 1, 2, 3 \dots 24)$, under different preloads can be computed. Part of the tested values of the matrix, K_{11} , K_{22} , K_{33} , and K_{44} ,

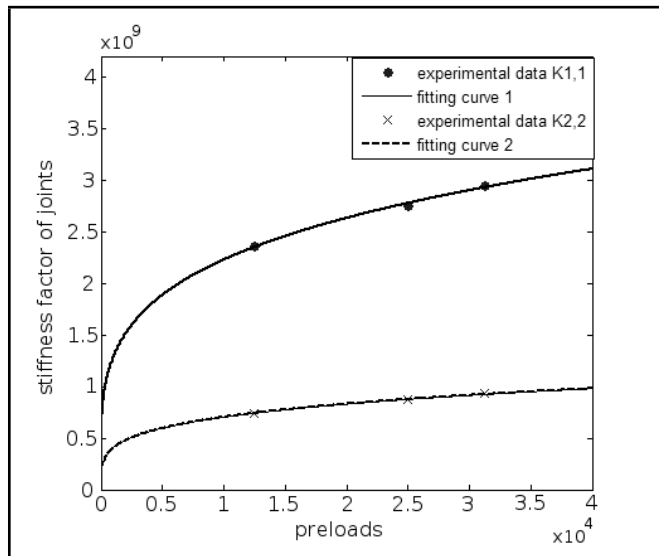


Figure 4: The relationship between the stiffness influence factors and the preloads:

$$K_{11} : c = 109477010.954254; d = 0.203506 \text{ and}$$

$$K_{22} : c = 109488536.164174; d = 0.203482.$$

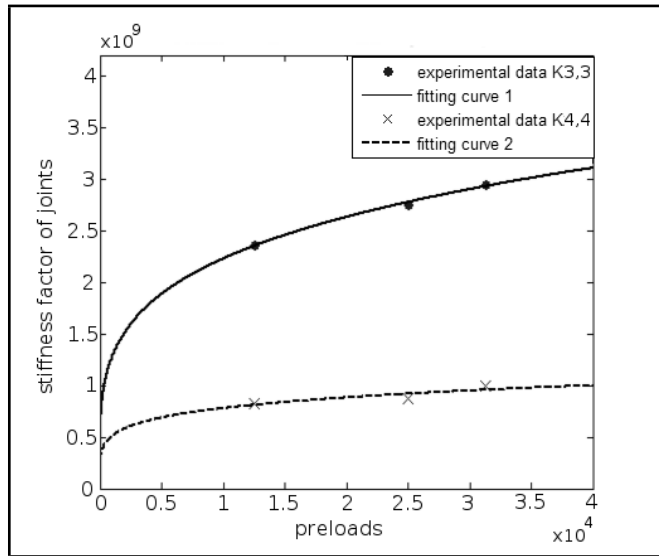


Figure 5: The relationship between the stiffness influence factors and the preloads:

$$K_{33} : c = 347156065.794277; d = 0.203482 \text{ and}$$

$$K_{44} : c = 167806537.456887; d = 0.166516.$$

are presented in Fig. 4 and Fig. 5. The least square method is employed in curve-fitting these test data, and the resulting curves are shown in Fig. 4 and Fig. 5. With these fitted curves, the stiffness coefficient K_{ij} of the bolted joint elements, under different preloads can be obtained without additional experiments. Therefore, this method greatly simplifies the modelling process of bolted joint elements.

2.3. Influence of Dimension on Dynamic Parameters

Experimental specimens were designed and manufactured for the research regarding the relationship between the dimensions of the joint surface and the value of the stiffness coefficient matrix $[K]$. The shape of these specimens is shown in Fig. 2 and the dimensions are listed in Table 1. There were 16

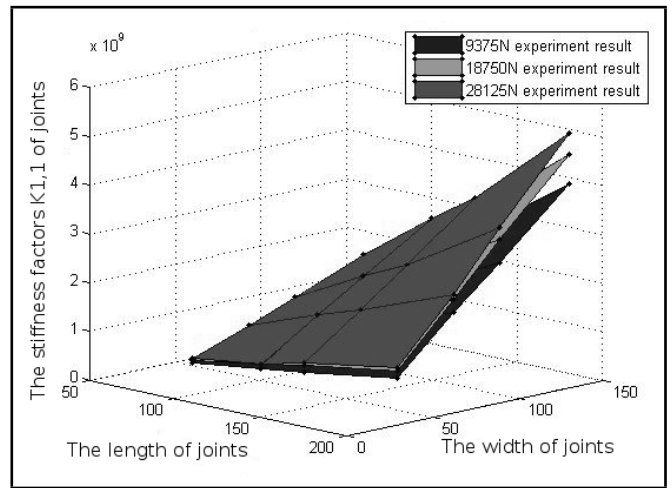


Figure 6: The experimental result of K_{11} in Ra 0.8.

specimens in all used during this research. With three preloads and two surface roughnesses, a total of 96 stiffness coefficient matrices $[K]$ were identified, which constituted the database of this work. The aforementioned method of the recognition of the stiffness matrix was used in this research.

Based on preliminary investigation, Response Surface Methodology (RSM) was introduced, to reveal the influence of the joint surface dimension on its dynamic characteristics. RSM¹¹ is a combination of mathematical and statistical technique, and is used in the empirical study of relationships between the independent variables/inputs $x_1, x_2, x_3 \dots x_n$ and the dependent variable/response Y . It is assumed that the independent variables are continuous and controllable within tolerance limits. The relationship between the response and inputs can be expressed as:

$$Y = F(x_1, x_2, x_3 \dots x_n) + e; \quad (5)$$

where Y is regarded as the response surface and e denotes the experimental error. The statistical model established by RSM gives a complete summary of the experimental results, and also enables the prediction of the values of factors that are not tested experimentally.

As shown in Fig. 6, every element of the joint stiffness matrix, with a certain roughness and preload, can be expressed as a saddle-like surface at the variation of length and width. As a result, a parameterized model of the stiffness matrix elements is established as:

$$z = \beta_0 + \beta_1 y x + \beta_2 y + \beta_3 x; \quad (6)$$

In Eq. (6), x and y represent the length and width, respectively, of the joint elements. z represents the corresponding stiffness matrix of joints. $\beta_k (k = 0, 1, 2, 3)$ is the impact parameter matrix of joints with certain surface roughness and preloads, which can be determined from the least square approximation to experimental results, as shown in Fig. 6 and Fig. 8 (e.g., recording the experimental results of the element K_{11} in the stiffness matrix); subsequently, the parameterized model of joints can be obtained.¹²

Taking the solving process of one element Z^{ij} in a z -matrix as an example, this paper describes how one single element $\hat{\beta}_k^{ij}$ in the corresponding β_K -matrix ($k = 0, 1, 2, 3$) is determined individually. Based on the least square method, there is the

Table 1: Dynamic-experiment specimens and the corresponding working conditions.

Experimental specimens	Interface dimension ($a \times b$; Unit: mm)	Substructure dimension ($l \times w \times h$; Unit: mm)	Preload F_N	Surface roughness
1	80 × 30	230 × 100 × 260	9375N	Ra 1.6 (precisely milling)
2	80 × 63	230 × 180 × 260		
3	80 × 90	230 × 230 × 260		
4	80 × 130	230 × 250 × 260		
5	120 × 30	240 × 100 × 260		
6	120 × 63	240 × 180 × 260		
7	120 × 90	240 × 230 × 260	18750N	Ra 0.8 (grinding)
8	120 × 130	240 × 150 × 260		
9	145 × 30	270 × 100 × 260	28125N	Ra 0.8 (grinding)
10	145 × 63	270 × 180 × 260		
11	145 × 90	270 × 230 × 260		
12	145 × 130	270 × 250 × 260		
13	200 × 30	320 × 100 × 260		
14	200 × 63	320 × 180 × 260		
15	200 × 90	320 × 230 × 260		
16	200 × 130	320 × 250 × 260		

Table 2: The dimensions of the joint interfaces.

Number	1	2	3	4	5	6	7
			(2 in all)	(2 in all)	(2 in all)	(2 in all)	
Interface dimension (length × width; Unit: mm)	210 × 88	320 × 88	144 × 88	215 × 88	265 × 88	201 × 88	250 × 88

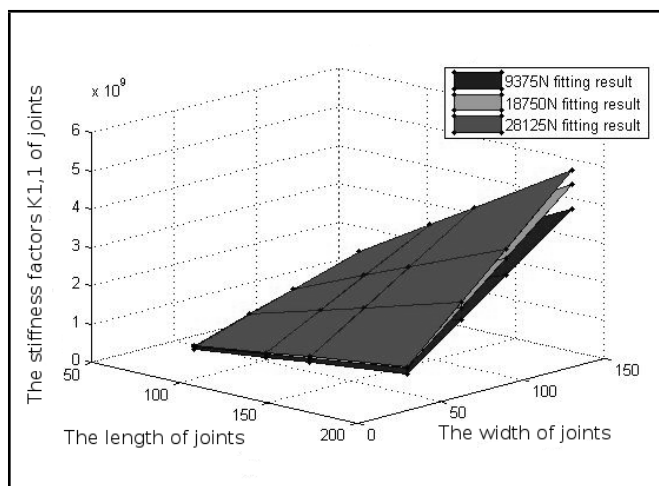


Figure 7: The regression analysis result of K_{11} in Ra 0.8.

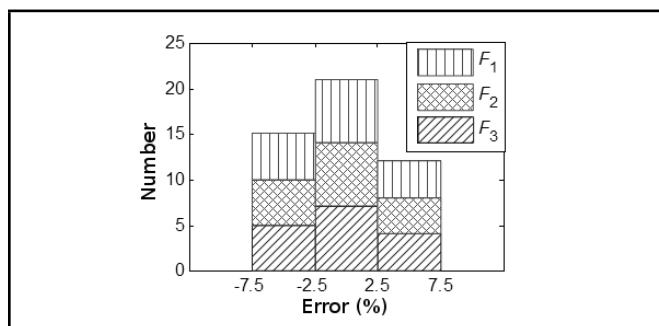


Figure 8: The error distribution of the fitted K_{11} .

following Eq. 7, where

$$\frac{\partial Q}{\partial \hat{\beta}_0^{ij}} = 0; \frac{\partial Q}{\partial \hat{\beta}_1^{ij}} = 0; \frac{\partial Q}{\partial \hat{\beta}_2^{ij}} = 0; \frac{\partial Q}{\partial \hat{\beta}_3^{ij}} = 0. \quad (8)$$

In the above formula, x_p , and y_q represent the length and width of the joint elements, respectively, and N indicates the

number of these dimensions, while Z_{ij} is a certain element of the corresponding matrix.

Expanding Eq. 8 produces the following Eq. 9.

Here, $\hat{\beta}_0^{ij}$, $\hat{\beta}_1^{ij}$, $\hat{\beta}_2^{ij}$, and $\hat{\beta}_3^{ij}$ can be obtained. Similarly, according to Eqs. (7) (9), the other elements of the β_i -matrix may be calculated, and then the other elements of the z-matrix are obtained.

Based on the dynamic parameterized model defined in Eq. (6), the authors work out the dynamic matrices of the joint elements with surface roughness Ra0.8 and different preloads. Fig. 6 and Fig. 7 compare the simulation results from the dynamic parameterized models against the experimental results, with a relative error of less than 7.5 %. Furthermore, the reflected relationship between the elements of the stiffness matrix and the influence factors also correlates with the experimental results. The above discussion shows the effectiveness of the established dynamic parameterized models.¹ Fig. 8 compares the experiments results and the RSM results using K_{11} as an example.

2.4. Influence of Surface Roughness on Dynamic Parameters

Surface roughness is one of the basic quality evaluation criteria, and plays an important role in joint dynamics. Extensive survey results show that such surface roughness as Ra0.8 and Ra1.6 were the most common requirements labelled in drawing designs. In order to study the influence of surface roughness on joints, several specimens with the same structure were made according to different ranks of roughness, which can be seen in Table 1. In each case of surface roughness, the effect of the bolt pre-tightening force and the interface dimensions on the joint dynamics was analysed in the same way as mentioned above, and a similar conclusion was obtained.

The parameters in Eq. (6) were determined by experimental results, and then the whole parameterized model was estab-

$$Q = \min \left\{ \sum_{p=1}^N \sum_{q=1}^N (Z^{ij} - \hat{\beta}_0^{ij} - \hat{\beta}_1^{ij} y_q x_p - \hat{\beta}_2^{ij} y_q - \hat{\beta}_3^{ij} x_p)^2 \right\}; \quad (7)$$

$$\begin{cases} -2 \sum_{p=1}^N \sum_{q=1}^N (Z^{ij} - \hat{\beta}_0^{ij} - \hat{\beta}_1^{ij} y_q x_p - \hat{\beta}_2^{ij} y_q - \hat{\beta}_3^{ij} x_p) = 0 \\ -2 \sum_{p=1}^N \sum_{q=1}^N (Z^{ij} - \hat{\beta}_0^{ij} - \hat{\beta}_1^{ij} y_q x_p - \hat{\beta}_2^{ij} y_q - \hat{\beta}_3^{ij} x_p) \cdot x_p \cdot y_q = 0 \\ -2 \sum_{p=1}^N \sum_{q=1}^N (Z^{ij} - \hat{\beta}_0^{ij} - \hat{\beta}_1^{ij} y_q x_p - \hat{\beta}_2^{ij} y_q - \hat{\beta}_3^{ij} x_p) \cdot y_q = 0 \\ -2 \sum_{p=1}^N \sum_{q=1}^N (Z^{ij} - \hat{\beta}_0^{ij} - \hat{\beta}_1^{ij} y_q x_p - \hat{\beta}_2^{ij} y_q - \hat{\beta}_3^{ij} x_p) \cdot x_p = 0 \end{cases} \quad (9)$$

lished. With that model, the authors were able to calculate the stiffness matrix of the joints of any dimension in terms of length and width, with the given roughness and preload. Subsequently, dynamic models can be set up¹³ to provide basic data for the quick and accurate modelling of machine tools, without any additional experiment or parameter identification.

3. THE PROCESS OF THE PARAMETERIZED DYNAMIC MODELLING METHOD

3.1. Data Base for Bolted Joint Modelling

According to previous work⁹ and taking the influence factors of joints dynamic characteristics into account comprehensively, a series of dynamic experiment specimens were designed considering different working conditions. There are 16 different dimensions listed in Table 1, which include three preloads and two interface roughnesses.

Each specimen listed in Table 1 is composed of two sub-structures connected with bolts, as shown in Fig. 2. Benefitting from a past approach,⁹ this paper carries out 96 experiments (as seen in Table 1) and resulted in the dynamic stiffness influence coefficient matrices of the specimens joints.

These 96 matrices constituted the foundation for modelling the bolted joint of the arbitrary dimension and preloads, with certain interface roughness.

3.2. Modelling Process

The process of bolted joint modelling is illustrated in Fig. 9.

First, the interface roughness requirement was obtained from the drawing designs. It is guaranteed that the interface roughness is Ra 0.8, Ra 1.6, or other discrete values. Then, corresponding matrices were selected as the modelling foundation from the database mentioned above.

Second, and for the joint element of each dimension shown in Table 1, there were 24×24 elements for constituting the stiffness matrix. For every element, e.g., K_{11} , a fitted curve was drawn out according to the element values of the same location in the three matrices selected above, corresponding to three preloads separately. On the basis of this curve, the value of K_{11} corresponding to the real preload was determined. The same steps were repeated for the other elements of this matrix. Therefore, all 16 matrices were obtained.

Third, for every element in the stiffness matrix $[K]$, there were 16 fitted values corresponding to 16 different joint dimensions, according to the 16 matrices mentioned above. Based on these 16 curves, the parameterized model of the stiffness matrix elements (such as K_{11}) was set up. Then, this model provided the value of K_{11} , corresponding to the actual dimensions of the modelled joint element. In this way, the other elements

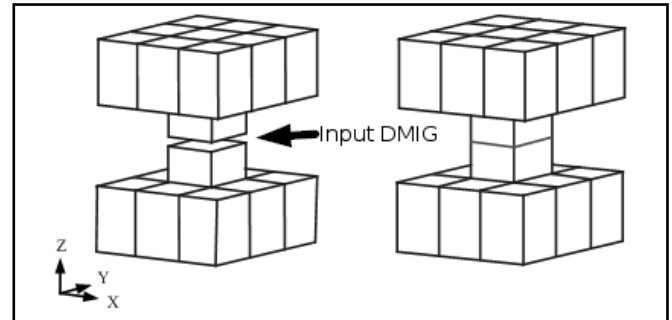


Figure 10: The model assembly process.

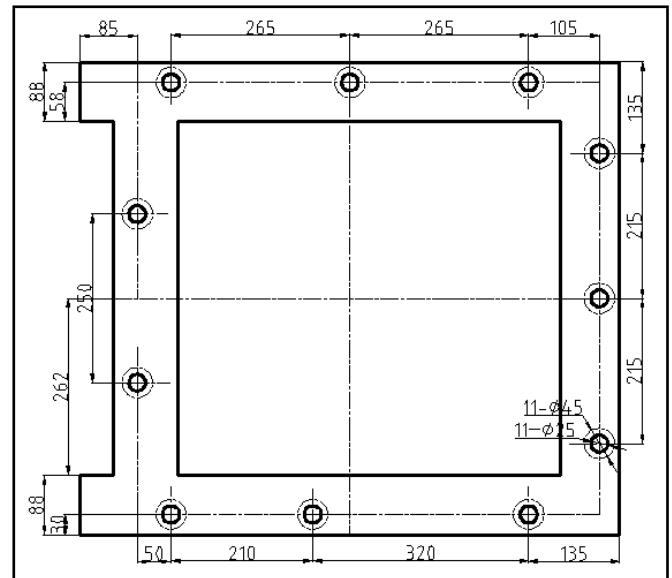


Figure 11: The dimension of the 'pane model'.

of the matrix were easily computed. When the stiffness matrix of the modelled joint element was obtained, the dynamic characteristics were revealed.

Finally, the stiffness matrix of the bolted joints was uploaded into the Direct Matrix Input at Grid (DMIG) card of MSC Nastran, and it was assembled with the FEM models of the two sub-structures. As a result, the dynamic model of the whole structure was obtained. Fig. 10 shows the assembly process.

4. EXPERIMENTAL VERIFICATION

4.1. Pane Model Verification of the Bolted Joints between the Machine Column and Bed

A test-piece called a 'pane model' was made to imitate the bolted connection of the XHK5140 machine column and bed. The dimension of each substructure was $700\text{mm} \times 800\text{mm} \times$

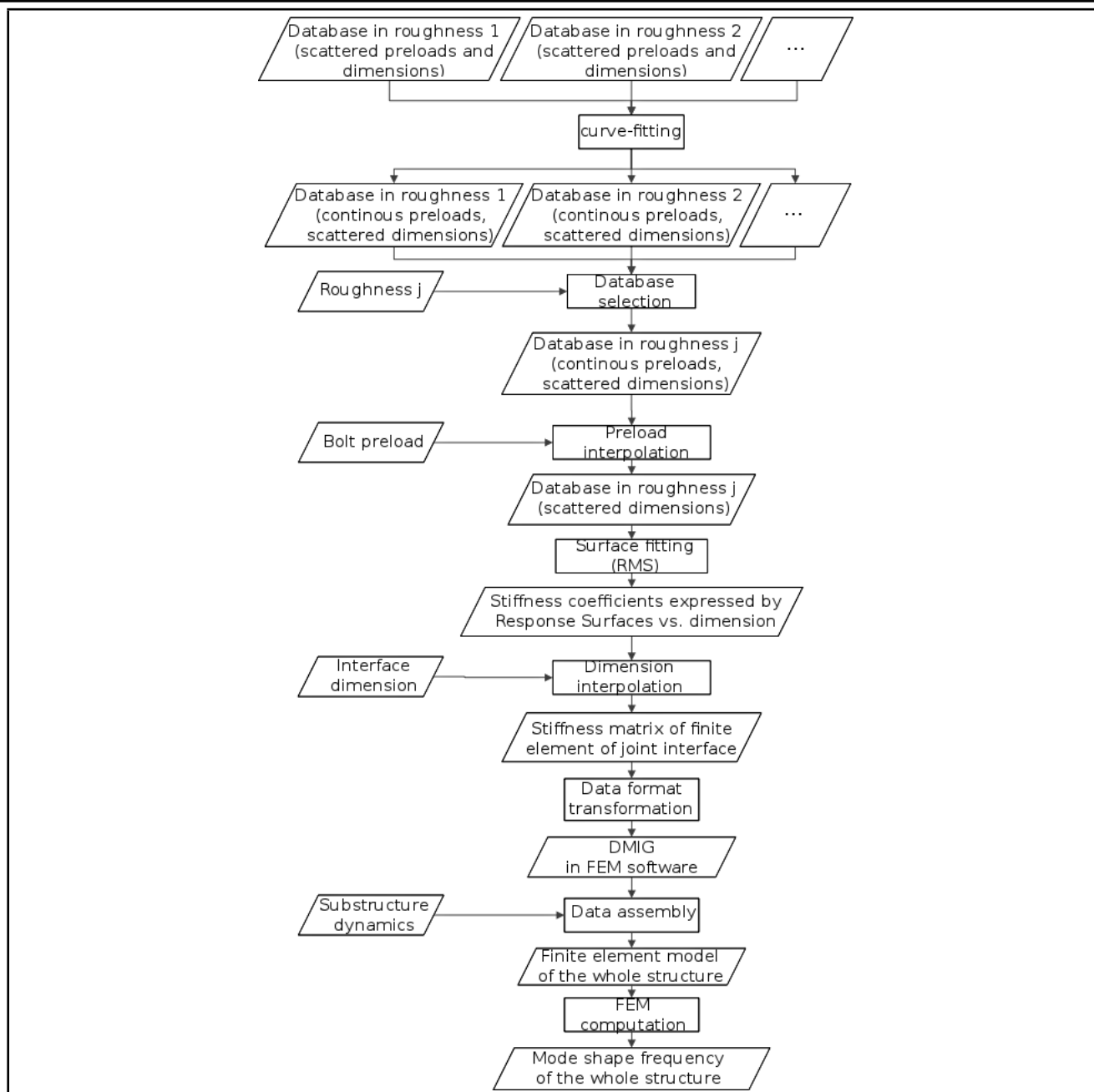


Figure 9: The modelling process .

50mm, the required roughness of the joint surfaces by the drawing was Ra 1.6, and 11 bolts (M24) were used to connect the joint. Additionally, the preloads were $F_1 = 9375N$, $F_2 = 18750N$, and $F_3 = 28125N$ in successive experiments. As shown in Fig. 12 and Fig. 13, the structure material was HT250. The other parameters used are listed as follows: the Elastic modulus $E = 1.16e11Pa$, Poisson's ratio: $\gamma = 0.27$, and the density: $\rho = 7340 \frac{kg}{m^3}$. The Single Input Multiple Output Method (SIMO) was used in the experiments.

The test site is shown in Fig. 12. During these experiments, model parameters, such as frequency with corresponding modal shape were obtained.

This model that was established omitted rounding chamfers, grooves and bolt holes, which subsequently resulted in a simplified finite element model of joint substructure with hexahedral finite elements by using MSC.FEA. The substructures were meshed with the elements boundaries, crossing the cen-

trelines of bolts.⁹ The final finite element model is shown in Fig. 13. In addition, convergence tests were conducted with the substructure FE model, and the results show that the size of the substructure finite elements in this work satisfied the requirement of simulation accuracy.

Besides the substructure finite element model, one joint element was built between every two bolts. Hence, there are altogether eleven joint elements, according to the drawing shown in Fig. 11. The dimension of every element is shown.

On the basis of the parameterized dynamic model presented in Eq. (6), the stiffness matrices of joints were calculated. For instance, the stiffness matrix of one joint element (dimension: 210×88 , $F_N = 18750N$) is:

$$K = \begin{bmatrix} K' & -K' \\ -K' & K' \end{bmatrix};$$

where detailed expression of K' is provided (on page 16).

$$K' = \begin{bmatrix} 2.0e9 & 2.4e5 & 4.0e7 & 1.1e9 & 2.0e4 & 3.2e6 & 5.2e8 & -2.5e5 & 1.7e6 & 1.0e9 & -2.0e4 & 2.1e7 \\ 2.4e5 & 2.0e9 & 2.2e7 & -1.9e4 & 1.0e9 & 1.1e7 & -2.4e5 & 5.1e8 & 9.7e5 & 1.9e4 & 1.0e9 & 1.8e6 \\ 4.0e7 & 2.2e7 & 6.6e9 & -3.2e6 & 1.2e7 & 3.2e9 & -1.7e6 & -9.0e5 & 1.7e9 & 2.1e7 & -1.8e6 & 3.2e9 \\ 1.1e9 & -1.9e4 & -3.2e6 & 2.0e9 & -2.5e5 & -4.0e7 & 1.1e9 & 2.0e4 & -2.1e7 & 5.2e8 & 2.5e5 & -1.7e6 \\ 2.0e4 & 1.0e9 & 1.2e7 & -2.5e5 & 2.0e9 & 2.4e7 & -1.9e4 & 1.0e9 & 1.9e6 & 2.3e5 & 5.1e8 & 9.7e5 \\ 3.2e6 & 1.1e7 & 3.2e9 & -4.0e7 & 2.4e7 & 6.3e9 & -2.0e7 & -1.8e6 & 3.3e9 & 1.6e6 & -8.9e5 & 1.7e9 \\ 5.2e8 & -2.4e5 & -1.7e6 & 1.1e9 & -1.9e4 & -2.0e7 & 2.0e9 & 2.3e5 & -4.1e7 & 1.1e9 & 2.1e4 & -3.3e6 \\ -2.5e5 & 5.1e8 & -9.0e5 & 2.0e4 & 1.0e9 & -1.8e6 & 2.3e5 & 2.0e9 & -2.2e7 & -2.0e4 & 1.0e9 & -1.1e7 \\ 1.7e6 & 9.7e5 & 1.7e9 & -2.1e7 & 1.9e6 & 3.3e9 & -4.1e7 & -2.2e7 & 6.4e9 & 3.4e6 & -1.1e7 & 3.2e9 \\ 1.0e9 & 1.9e4 & 2.1e7 & 5.2e8 & 2.3e5 & 1.6e6 & 1.1e9 & -2.0e4 & 3.4e6 & 2.0e9 & -2.5e5 & 4.2e7 \\ -2.0e4 & 1.0e9 & -1.8e6 & 2.5e5 & 5.1e8 & -8.9e5 & 2.1e4 & 1.0e9 & -1.1e7 & -2.5e5 & 2.1e9 & -2.3e7 \\ 2.1e7 & 1.8e6 & 3.2e9 & -1.7e6 & 9.7e5 & 1.7e9 & -3.3e6 & -1.1e7 & 3.2e9 & 4.2e7 & -2.3e7 & 6.3e9 \end{bmatrix}$$



Figure 12: The experiment with the 'pane model'.

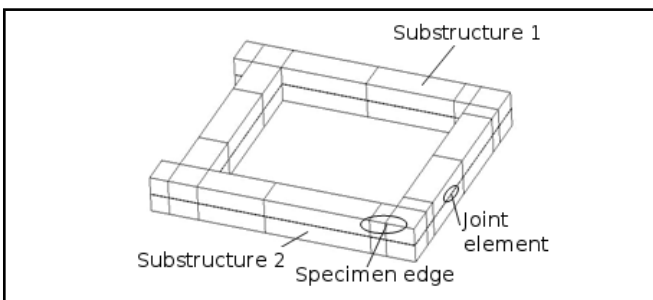


Figure 13: The FEM of the 'pane model'.

Likewise, the stiffness matrix of joints can be worked out under any preload, while the roughness is $1.6\mu\text{m}$. This stiffness matrix was inputted into the DMIG card of MSC Nastran. It was then assembled with the stiffness matrix of each sub-structure, and then the stiffness matrix of the whole structure was obtained. Finally, based on modal analysis of the whole-structure dynamic model, modal parameters were observed (calculated results). On the basis of having the same mode shapes, the calculated results and experimental results are compared, as shown in Table 3 and Table 4.

The results of Table 3 and Table 4 show that the difference between simulation and experiment results is small and that the first five mode shapes are in perfect accordance. These results

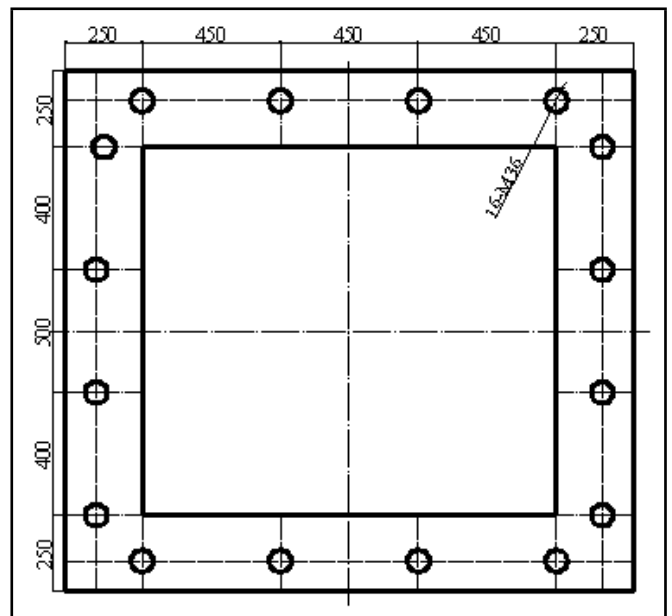


Figure 14: The geometric dimensions of fixed joints and distribution of bolts.

validate the effectiveness of this parameterized dynamic model for bolted joints presented in this paper.

4.2. Verifying with the CKX5680 Machine Tool

For a CKX5680 machine tool with seven-five axis made by W.Z. (a heavy machine tool factory in China), there are 16 bolts (M36) used to connect beams and columns. The geometric dimensions of the bolted joints and the distribution of bolts are shown in Fig. 14. The roughness of those joints is $1.6\mu\text{m}$. The moment of pre-tightening force is 500Nm . The material of the beam and the column is HT250. Other parameters are listed as follows: the elastic modulus: $E = 1.2e11\text{Pa}$, Poisson's ratio: $\gamma = 0.27$, and the density: $\rho = 7500 \frac{\text{kg}}{\text{m}^3}$.

On one hand, with the experiment modal analysis of this machine through the SIMO method, the preceding five modal shapes were observed. The testing site is shown in Fig. 15.

On the other hand, the finite element model of the whole machine tool can be established according to the procedure that follows. First, according to the drawing sketch of the machine tool, the FE model with the hexahedral finite elements of every single part of that structure is established separately, e.g., the column, the beam and so on. The finite element model is

Table 3: A comparison of the calculated results and the experimental results.

Preload	Result	1 st mode	2 nd mode	3 rd mode	4 th mode	5 th mode
9375N	Experimental result (Hz)	166.286	244.387	403.191	597.753	806.227
	Calculated result (Hz)	167.45	247.82	398.33	595.62	882.02
	Percentage error (%)	0.7	1.40	-1.21	-0.36	9.40
18750N	Experimental result (Hz)	172.636	244.449	403.061	611.324	806.123
	Calculated result (Hz)	169.09	247.84	398.33	597.21	882.08
	Percentage error (%)	-2.05	1.39	-1.17	-2.31	9.42
28125N	Experimental result (Hz)	177.669	244.642	403.284	621.468	807.018
	Calculated result (Hz)	170.02	247.85	398.34	598.2	882.08
	Percentage error (%)	-4.31	1.31	-1.23	-3.74	9.30



Figure 15: The test site of the modal experiments.

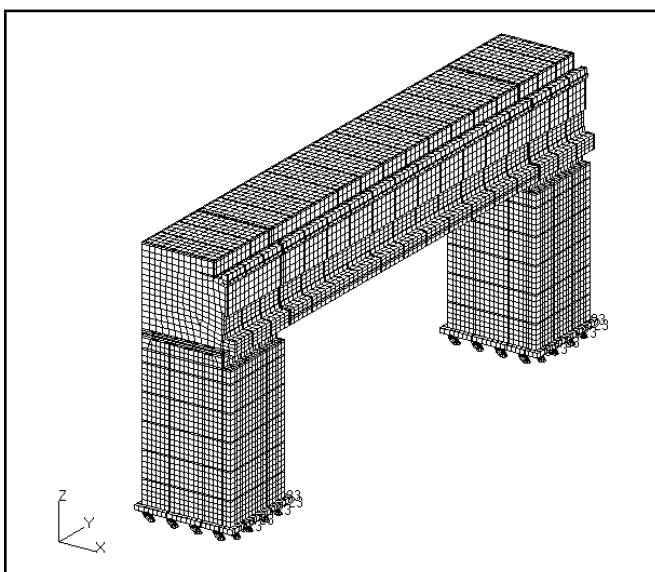


Figure 16: The FEM of CKX5680.

shown in Fig. 16.¹⁴

Second, the finite element models of the bolted joint between every two bolts are built, and there are 16 elements in total. Table 6 lists the dimensions of every bolted joint element.

According to the parameterized dynamic model for bolted joints presented in Eq. (6), the stiffness matrix could be worked out in the situation that the roughness is $1.6\mu\text{m}$ and the pre-tightening force is 500Nm . Following this, the stiffness matrix was entered into the DMIG card in MSC Nastran, and assembled with the stiffness matrix of the other component units; as a result, the dynamic model of the whole machine tool was obtained. Finally, with the model analysis of the whole-structure

dynamic model, the modal parameters needed were obtained through calculated results. Under the standard of modal shape agreement, calculated results and experimental results were compared, and final results are shown in Table 5.

The results in Table 5 show that the differences between the simulation results and the experiment results are very small, while the modal shapes of the first five modes are in accordance. These experiments validate the effectiveness of the parameterized dynamic model of fixed joints presented in this paper.

Although part of the simulation errors reached up to 20 %, the accuracy of the proposed method is still higher than that of others, such as the Yoshimura method and spring-damping method. A mesh convergence test showed that the influence of the element size on the simulation results can be ignored. The error may be a result of: 1) the data processing during the modal tests, or 2) the actual preload of the joints not being able to determined exactly from the tightening torque of bolts with the empirical formulas.

5. CONCLUSIONS

Based on the analysis of the specimens, this paper presents a mathematic dynamic modelling method of bolt joints, employing the curve-fitting method and Response Surface Methodology. For a given bolted structure (material HT250), one can establish the finite element model of its joint—specifically the equivalent stiffness coefficient matrix—using the sample database of joint models. Subsequently, the finite element model of the whole structure can be determined. Then, the modal frequencies and accurate mode shapes can be obtained.

The influence of the bolt pre-tightening force and interface dimensions on the dynamic characteristics of the joints of designed specimens was analysed in detail. Two major results were found: (1) for every stiffness coefficient in the joints finite element model, its value can be expressed as an exponential function of the bolt pre-tightening force with other conditions unchanged; and (2) similarly, every stiffness coefficient can be expressed as a quadratic function of interface dimensions, namely the length and the width. Furthermore, the same bolted joint database in each case of roughness was established separately, revealing the same results mentioned above.

Through the dynamic experiments on the *pane model* and the machine tool with the seven-five axis, the experimental results of dynamic parameters were observed. Based on the parameterized model, the calculated results were obtained and entered into the finite element model of the whole structure. A comparison of the two shows that the simulation results agreed very well with the experiments and most of the errors are less

Table 4: A comparison between the calculated and the experimental results (preload $F_2 = 18750N$).

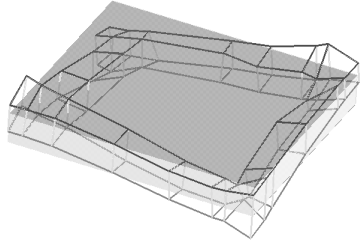
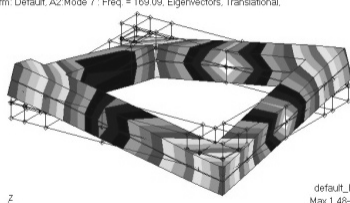
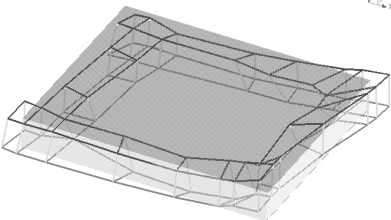
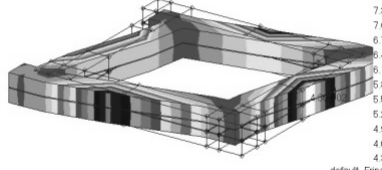
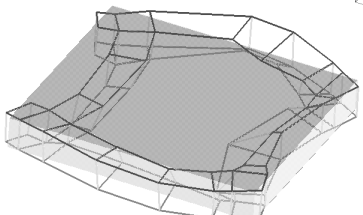
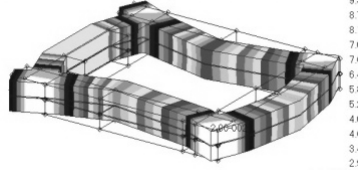
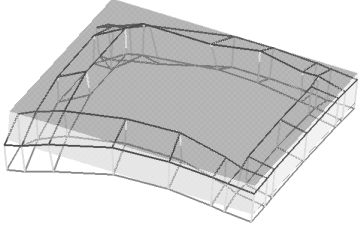
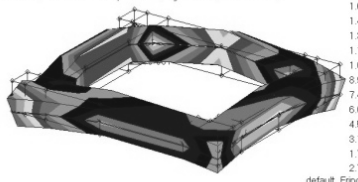
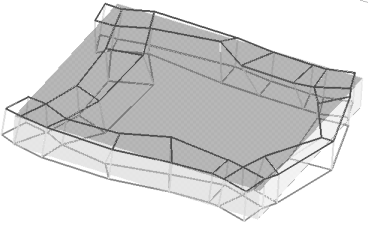
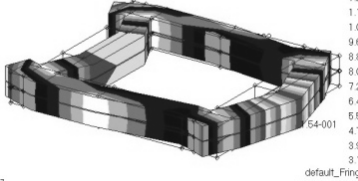
Order	Experimental mode shapes	Calculated mode shapes
1	 <p>Modal frequency: 172.636 Hz</p>	 <p>MSC.FEA 2005 r2 20-Jul-10 10:19:05 Fringe: Default, A2, Mode 7 : Freq = 169.09, Eigenvectors, Translational, Magnitude, (NON-LA...) Deform: Default, A2, Mode 7 : Freq = 169.09, Eigenvectors, Translational.</p> <p>Modal frequency: 169.09 Hz; error (-2.05%)</p>
2	 <p>Modal frequency: 244.449 Hz</p>	 <p>MSC.FEA 2005 r2 20-Jul-10 10:22:41 Fringe: Default, A2, Mode 8 : Freq = 247.84, Eigenvectors, Translational, Magnitude, (NON-LA...) Deform: Default, A2, Mode 8 : Freq = 247.84, Eigenvectors, Translational.</p> <p>Modal frequency: 247.84 Hz; error (1.39%)</p>
3	 <p>Modal frequency: 403.061 Hz</p>	 <p>MSC.FEA 2005 r2 20-Jul-10 10:23:11 Fringe: Default, A2, Mode 9 : Freq = 398.33, Eigenvectors, Translational, Magnitude, (NON-LA...) Deform: Default, A2, Mode 9 : Freq = 398.33, Eigenvectors, Translational.</p> <p>Modal frequency: 398.33 Hz; error (-1.17%)</p>
4	 <p>Modal frequency: 611.324 Hz</p>	 <p>MSC.FEA 2005 r2 20-Jul-10 10:25:57 Fringe: Default, A2, Mode 11 : Freq = 597.21, Eigenvectors, Translational, Magnitude, (NON-LA...) Deform: Default, A2, Mode 11 : Freq = 597.21, Eigenvectors, Translational.</p> <p>Modal frequency: 597.21 Hz; error (-2.31%)</p>
5	 <p>Modal frequency: 806.123 Hz</p>	 <p>MSC.FEA 2005 r2 20-Jul-10 10:26:30 Fringe: Default, A2, Mode 15 : Freq = 882.05, Eigenvectors, Translational, Magnitude, (NON-LA...) Deform: Default, A2, Mode 15 : Freq = 882.05, Eigenvectors, Translational.</p> <p>Modal frequency: 882.08 Hz; error (9.42%)</p>

Table 5: A comparison between the modal shapes of calculated and experimental results.

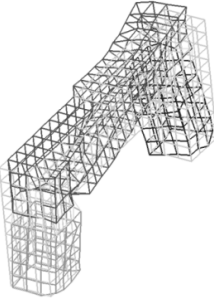
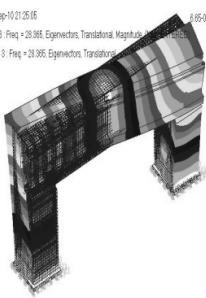
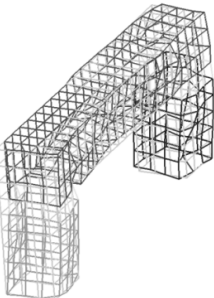
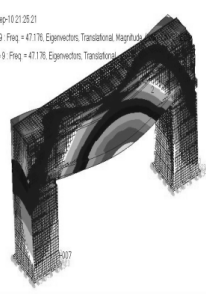
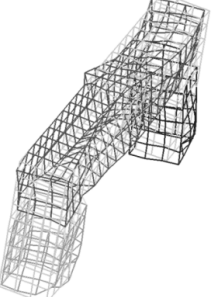
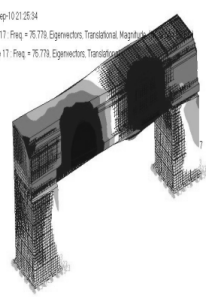
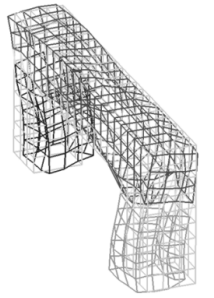

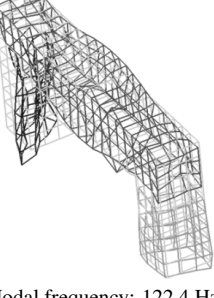
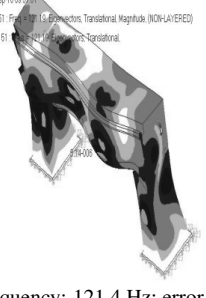
Order	Modal shape in experimental result	Modal shape in calculated result
1	 <p>Modal frequency: 23.8 Hz</p>	 <p>Modal frequency: 28.4 Hz; error (19.33%)</p>
2	 <p>Modal frequency: 44.8 Hz</p>	 <p>Modal frequency: 47.2 Hz; error (5.36%)</p>
3	 <p>Modal frequency: 72.4 Hz</p>	 <p>Modal frequency: 75.8 Hz; error (4.70%)</p>
4	 <p>Modal frequency: 81.4 Hz</p>	 <p>Modal frequency: 80.1 Hz; error (-1.60%)</p>
5	 <p>Modal frequency: 122.4 Hz</p>	 <p>Modal frequency: 121.4 Hz; error (-0.82%)</p>

Table 6: The dimensions of every bolted joint element in CKX5680.

Number	1 (2 in all)	2 (4 in all)	3 (6 in all)	4 (4 in all)
Interface dimension (length × width; Unit: mm)	500 × 250	400 × 250	450 × 250	212 × 250

than 10 % (rarely > 10 %). The results prove that the parameterized models of joints are accurate and effective in the dynamic modelling field.

ACKNOWLEDGEMENTS

This work was supported by grants from the Key Projects in the National Science & Technology Pillar Program (No. 2012BAF08B01) and the Major State Basic Research Development Program of China (No. 2011CB706803). The authors are grateful to other participants of the projects for their cooperation, particularly Hongliang Tian.

REFERENCES

- Greenwood, J. A., and Williamson, J. Contact of nominally flat surfaces. *Proceedings of the Royal Society of London. Series A. Mathematical and Physical Sciences*, **295**(1442), 300–319, (1966).
- Yoshimura, M. Making use of CAD technology based on the dynamic characteristics data of joints to improve the structural rigidity of machine tools. *Machine Tools*, **1**(1), 142–146, (1979).
- Greenwood, J. A., and Tripp, J. H. The elastic contact of rough spheres. *Journal of Applied Mechanics*, **34**, 153, (1967).
- Namazi, M., et al. Modeling and identification of tool holder–spindle interface dynamics. *International Journal of Machine Tools and Manufacture*, **47**(9), 1333–1341, (2007).
- Zhang, Y. and Liao, B. The Efficient Identification Method of Joint Parameters of Machine Tools. *Journal of Kunming University of Science and Technology*, **23**(2), 36–41, (1998).
- Tsai, J. and Chou, Y. The identification of dynamic characteristics of a single bolt joint. *Journal of Sound and Vibration*, **125**(3), 487–502, (1988).
- Wang, J. H. and Liou, C. M. Identification of parameters of structural joints by use of noise-contaminated FRFs. *Journal of sound and vibration*, **142**(2), 261–277, (1990).
- Ren, Y. and Beards, C. F. Identification of 'effective' linear joints using coupling and joint identification techniques. *Journal of Vibration and Acoustics*, **120**(2), 331–338, (1998).
- Mao, K., et al. Stiffness influential factors-based dynamic modeling and its parameter identification method of fixed joints in machine tools. *International Journal of Machine Tools and Manufacture*, **50**(2), 156–164, (2010).
- Wen, S., et al. Fractal Model of Tangential Contact Stiffness of Joint Interfaces and Its Simulation. *Transactions of the Chinese Society for Agricultural Machinery*, (12), 223–227, (2009).
- Padmanabhan, K. K. Prediction of damping in machined joints. *International Journal of Machine Tools and Manufacture*, **32**(3), 305–314, (1992).
- Kim, T. R., Ehmann, K. F. and Wu, S. M., Identification of joint structural parameters between substructures. *Journal of engineering for industry*, **113**(4), 419–424, (1991).
- Padmanabhan, K. K. and Murty, A. Damping in structural joints subjected to tangential loads. *Proceedings of the Institution of Mechanical Engineers, Part C: Journal of Mechanical Engineering Science*, **205**(2), 121–129, (1991).
- Wang, S. and Huang, Y. The finite element analysis method of Machine tool characteristics. *Machine Tool and Hydraulics*, **2005**(03), 20–22, (2005).